Analysis of single and multi-objective optimization of the pultrusion process

Rita de Cassia Costa Dias, Lizandro de Sousa Santos

▶ **To cite this version:**

Rita de Cassia Costa Dias, Lizandro de Sousa Santos. Analysis of single and multi-objective optimization of the pultrusion process. Materials Today Communications, 2024, 35, pp.105677. 10.1016/j.mtcomm.2023.105677 . emse-04575946

HAL Id: emse-04575946

https://hal-emse.ccsd.cnrs.fr/emse-04575946v1

Submitted on 22 May 2024

HAL is a multi-disciplinary open access archive for the deposit and dissemination of scientific research documents, whether they are published or not. The documents may come from teaching and research institutions in France or abroad, or from public or private research centers.

L'archive ouverte pluridisciplinaire **HAL**, est destinée au dépôt et à la diffusion de documents scientifiques de niveau recherche, publiés ou non, émanant des établissements d'enseignement et de recherche français ou étrangers, des laboratoires publics ou privés.

Graphical Abstract

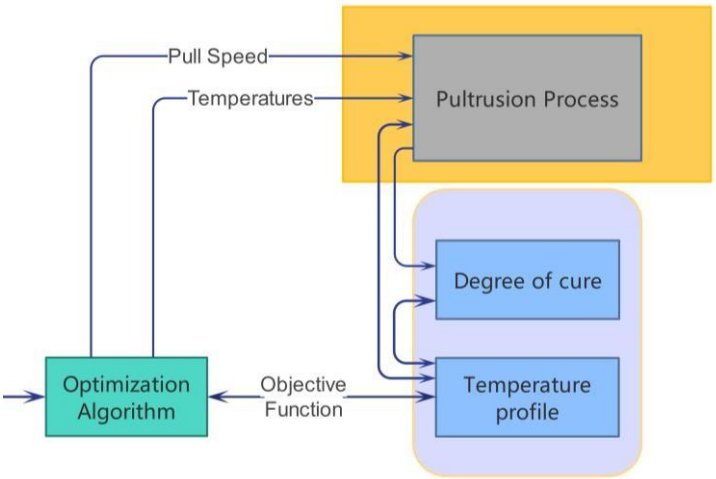

Manuscript File Click here to view linked References

Analysis of single and multi-objective optimization of the pultrusion process

Rita de Cassia Costa Dias[a], Lizandro de Sousa Santos[b]

[a]Department of Mechanics and Elaboration Processes, École des Mines de Saint-Étienne, 158, cours Fauriel, Saint-Étienne, 42100, France.

[b]Department of Chemical and Petroleum Engineering, Universidade Federal Fluminense, Rua Passo da Pátria, 156, CEP: 24210240, Niterói, RJ, Brazil.

Contact author: lizandrosousa@id.uff.br

Abstract

Understanding the cure reaction in the pultrusion process is essential to improve the quality of the pultruded composites and propose different design alternatives that contribute to improving the process performance. In this work, a computational strategy was used to optimize the pultrusion process, where the computational model was implemented into Ansys CFX® and the optimization algorithm was developed in the Matlab® software. Different optimization strategies applied to the two pultrusion processes simulated in the recent literature were investigated. For the optimization, we seek to minimize the sum of the temperatures of the pultrusion mold heaters, considering a minimum curing degree of 0.89. Particle swarm optimization (PSO) and sequential quadratic programming (SQP) algorithms were tested for single objective optimization. The results indicate that PSO presented lower objective-function values while the deterministic methods presented high sensitivity to the initial estimate of the optimization. The PSO algorithm was also used for multi-objective optimization of the process, in which the pull speed maximization and temperature minimization were defined as objective functions. It was possible to construct the Pareto curve, representing the set of optimal points of the process.

Keywords: Pareto, Polymer Composite, Nonlinear Programming

1. Introduction

Polymeric composites are manufactured by processes such as pultrusion, hand lay-up, filament winding, etc. The pultrusion consists of pulling a fiber set through a resin bath into a heated die where the part is cured. Outside the die, the composite part is pulled by a continuous pulling system and then a cut-off saw cuts the part into the desired length. Typically, the die is heated by electrical heaters coupled on its surface (Santos et al., 2015b).

Pultrusion is one of the few continuous processes to produce composite parts and allow the high-volume manufacture of structural profiles with improved mechanical properties and quality. Pultruded composites are widespread in numerous industries, including construction, transportation, consumer goods, and the electrical and chemical sector (Nickels, 2019). The development of models provides better knowledge regarding the mechanisms (cure kinetic) behind the process (Safonov et al., 2018).

Some researchers have studied the optimization of pultrusion in the last few years. Generally, the objectives are cost related, such as process time and energy consumption or quality-related, such as uniform degree of cure along the composite part. The constraints adopted include the maximum temperature allowed within the part to avoid degradation of the resin and the minimum degree of cure at the exit of the die (Struzziero et al., 2019).

The Simulated Annealing method was used by (Coelho and Calado, 2002) to optimize the pull speed of impregnated fibers and the temperature profile (boundary conditions) imposed on the die wall. Several constraints were considered, such as a minimum degree of cure and the thermal degradation condition. Li et al. (2002) implemented an optimization algorithm. The results evidenced that a uniformly cured part could be obtained with the optimization strategy. Joshi et al. (2003) (Joshi et al., 2003a) optimized the pultrusion system by applying a 3D finite element/nodal control volume. It was observed that during pultrusion, the die-cooler and pre-

heating system helped minimize the temperature overshoot within the composite. In the work of (Lam et al., 2003), optimization was realized to improve the production of a pultruded composite C-section. Die heating and pull speed were manipulated to enhance the degree of cure distribution, allowing an improvement of 52% in the uniformity of the degree of cure. In (Srinivasagupta and Kardos, 2004), a thermodynamic objective function was proposed to minimize the energy consumption during the cure reaction in an injection pultrusion process. The methodology determined the optimal values of the main parameters, such as temperatures, resin injection pressure and equipment specification. A one-stage optimization problem and multiperiod method were applied by (Acquah et al., 2006) to find the optimal cure temperature profile under uncertainty conditions for the pultrusion process. The authors observed that a few constraint violations reflect the need to use a global optimizer to satisfy the sufficiency conditions to reach the optimum solution. Carlone et al. (2007) (Carlone et al., 2007) employed a finite difference method to simulate the pultrusion process and subsequently proposed a hybrid approach combining the simplex method and genetic algorithms to improve the dimensional accuracy of fabricated parts. According to the authors, the distribution of the degree of cure at the die exit resulted in one of the main process parameters to obtain an optimized product. In previous work, Santos et al. (2012) (Santos et al., 2012) proposed a CFD (Computational Fluid Dynamic)-based optimization model to minimize the energy consumption of the pultrusion process. The algorithm was developed in a Fortran90 code coupled with the ANSYS CFX® software. It was possible to verify that the energy requirements could be reduced by changing the heating configuration of the pultrusion die. An alternative arrangement comprising internal heaters inside the die was proposed. Silva et al. (2014) investigated novel relative positions for the die heaters to optimize energy consumption. Finite Element Analysis (Chapra and Canale, 2003) was applied to identify the best relative position of the heaters into the die, considering the usual parameters involved in the process. In (Santos

et al., 2015b), a Particle Swarm Optimization (PSO) algorithm was used to optimize a cylindrical pultruded part. The partial differential equation (PDE) system was solved by the finite difference method (Chapra and Canale, 2003). The results revealed that the proposed strategy might be a good alternative to find the best operating point regarding energy cost. In (Costa et al., 2018), the pultrusion process of a glass fiber-epoxy set with different geometries was simulated by using a three-dimensional finite element-nodal control volume (FE/NCV) approach for simulating the process, whereas a quadratic programming algorithm and a PSO were used. In the work of Tutum et al. (2015), an optimization methodology based on the Kriging algorithm was introduced. The design problem involved a pultrusion die with one, two and three heaters. For optimization, the heaters and pull speed were selected as decision variables. The results showed that the proposed methodology efficiently finds the optimal design parameters. Tutum et al. (2013) used the nondominated sorting genetic algorithm (NSGA-II) to simultaneously maximize the pull speed and minimize the energy consumption associated with the temperatures. The methodology helped to design a pultrusion die for different operating conditions.

Recent work on pultrusion process optimization has revealed that the advancement of computational resources has facilitated the development of tools for the simulation and optimization of engineering processes. In pultrusion, finite element tools have been used for the 3D simulation of regular and irregular geometries. Generally, stochastic methods, such as particle swarm optimization and genetic algorithms, have been used for optimization. In fact, there are optimization processes of industrial interest that involve functions that present many local solutions. Therefore it is challenging to determine the optimal solution using deterministic optimization techniques.

Table 1 summarizes the main contributions concerning the optimization of the pultrusion process.

Table 1. Summary of the main contributions concerning the optimization of the pultrusion process.

Reference	OA	SOO	MOO
(Coelho and Calado, 2002)	SA	✓	
(Joshi et al., 2003b)	SD	✓	
(Lam et al., 2003)	SD	✓	
(Carlone et al., 2007)	SIMPLEX; GA	✓	
(Santos et al., 2009)	PSO		✓
(Tutum et al., 2013)	NSGA-II		✓
(Tutum et al., 2014)	NSGA2		✓
(Santos et al., 2015a)	PSO	✓	
(Costa et al., 2018)	CPLEX	✓	

In this work, we have developed a computational tool for single-objective and multi-objective optimization of the pultrusion process. The simulation was developed in Ansys CFX® software, while optimization was developed in the Matlab2022® environment. The tool is an improvement of the strategy developed in the previous works of Santos et al. (2009), where Fortran90 was used as an optimization tool.

2. Optimization

2.1 General Description

Optimization has found widespread use in the chemical engineering field. Problems in this area often have many alternative solutions with complex economic and performance interactions, so it is often not straightforward to identify the optimal solution through intuitive reasoning (Biegler, 2010; Nocedal, 1999).

The following system represents a general optimization problem:

$$min_{\mathbf{x}} f(x) \tag{1}$$

s.t.

$$h_j(\mathbf{x}) = 0; j = 1, \dots, m_e \tag{1a}$$

$$g_j(\mathbf{x}) \leq 0; j = 1, \dots, m_i \tag{1b}$$

$$\mathbf{x}_{min} \leq \mathbf{x} \leq \mathbf{x}_{max} \tag{1c}$$

Where f, g and h refer to the objective function, inequality constraints and equality constraints, respectively, m_i refers to inequality constraints while m_e refers to equality constraints. x_i, $i = 1 \cdots n_x$ are the decision variables and n_x is the number of decision variables.

2.2 Multi-objective optimization (MOO)

In Multi-objective optimization (MOO), the objectives are represented by two or more objective functions. In this way, equation (1) can be written according to equation (2):

$$\min_{\mathbf{x}}[f_1(x), f_2(x), \cdots, f_N(x)] \quad (2$$

The representation of a MOO with two objective functions is sketched in Fig. 1.

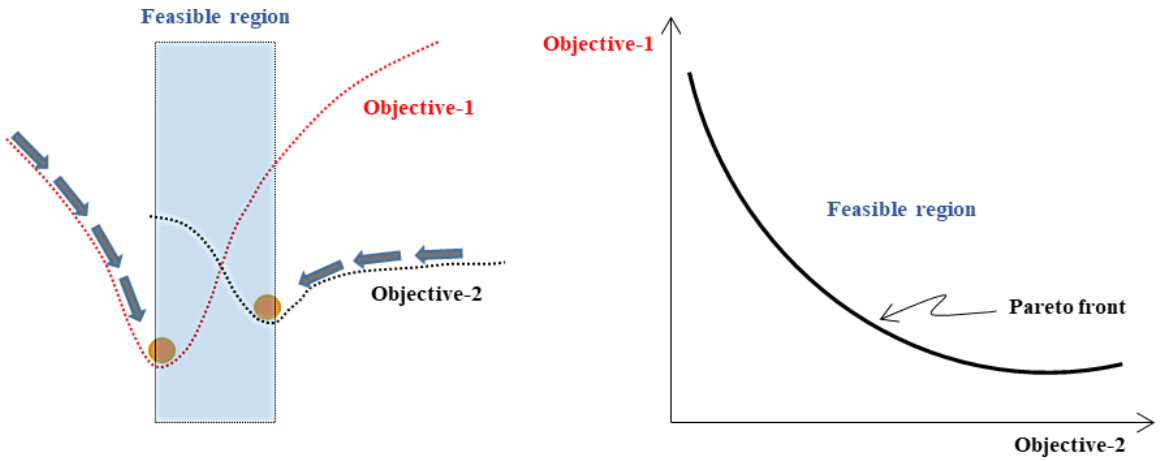

Fig.1. Representation of a MOO with two objective functions (minimization): 1(a) – left, 1(b) right.

Notice in Fig. 1(a) that there is a feasible region between the two minimum points of objective functions, and this region depends on the weights assigned to each function. Fig. 1(b) shows the Pareto front resulting from different assigned weights.

A MOO problem generally has two or more objectives involving decision variables and constraints. The mathematical formulation of a MOO with two objectives is given by equation 3(a-f):

$$\min_{\mathbf{x}\in\mathbb{R}^{n_x}} f_1(\mathbf{x}) \quad (3a)$$

$$\min_{\mathbf{x}\in\mathbb{R}^{n_x}} f_2(\mathbf{x}) \quad (3b)$$

$$s.t. \quad (3c)$$

$$\mathbf{x}_{min} \leq \mathbf{x} \leq \mathbf{x}_{max} \quad (3d)$$

$$g_j(\mathbf{x}) \leq \mathbf{0}, \ j = 1, \cdots, m_i \quad (3e)$$

$$h_j(\mathbf{x}) = \mathbf{0}, \ j = 1, \cdots, m_e \quad (3f)$$

The solutions of a MOO problem are known as the Pareto-optimal solutions. The following definition characterizes the Pareto-optimal solution:

Definition: The set: $\mathbf{x}^*$, $f_1(\mathbf{x}^*)$, $f_2(\mathbf{x}^*)$ is said to be the Pareto-optimal solution for the two-objective problem in equation (1) if, and only if, no other feasible $\mathbf{x}$ exists such that $f_1(\mathbf{x}) \leq f_1(\mathbf{x}^*)$ and

$f_2(\mathbf{x}) \leq f_2(\mathbf{x}^*)$ with strictly inequality valid for at least one objective (Pardalos et al., 2017).

For solving the MOO problem the weighted sum method may be applied:

$$\min \ \phi \frac{f_1(\mathbf{x}) - f_1^{min}}{f_1^{max} - f_1^{min}} + (1 - \phi) \frac{f_2(\mathbf{x}) - f_2^{min}}{f_2^{max} - f_2^{min}} \quad (4)$$

Where ϕ is the weighting factor and the superscripts min and max refer to the minimum and maximum values of objective functions. These vector components are used for normalizing the objectives, which are likely to have significantly different magnitudes in applications.

2.3 Numerical Implementation

This paper aims to show the advances obtained regarding the previous research of Santos et al. (2012, 2014), in which the optimization and communication with the Ansys CFX® simulator were developed in a Fortran90 code. Fig. 2 summarizes the optimization strategy. The simulation-optimization are performed cyclically, in which the temperature profiles and degree of cure are sent to the optimizer. After the objective function's evaluation, the computed values of decision variables are sent back to the simulator to perform a new iteration. Fig. 3 illustrates the structure of the Matlab-Ansys® CFX® communication, described by Algorithm 1.

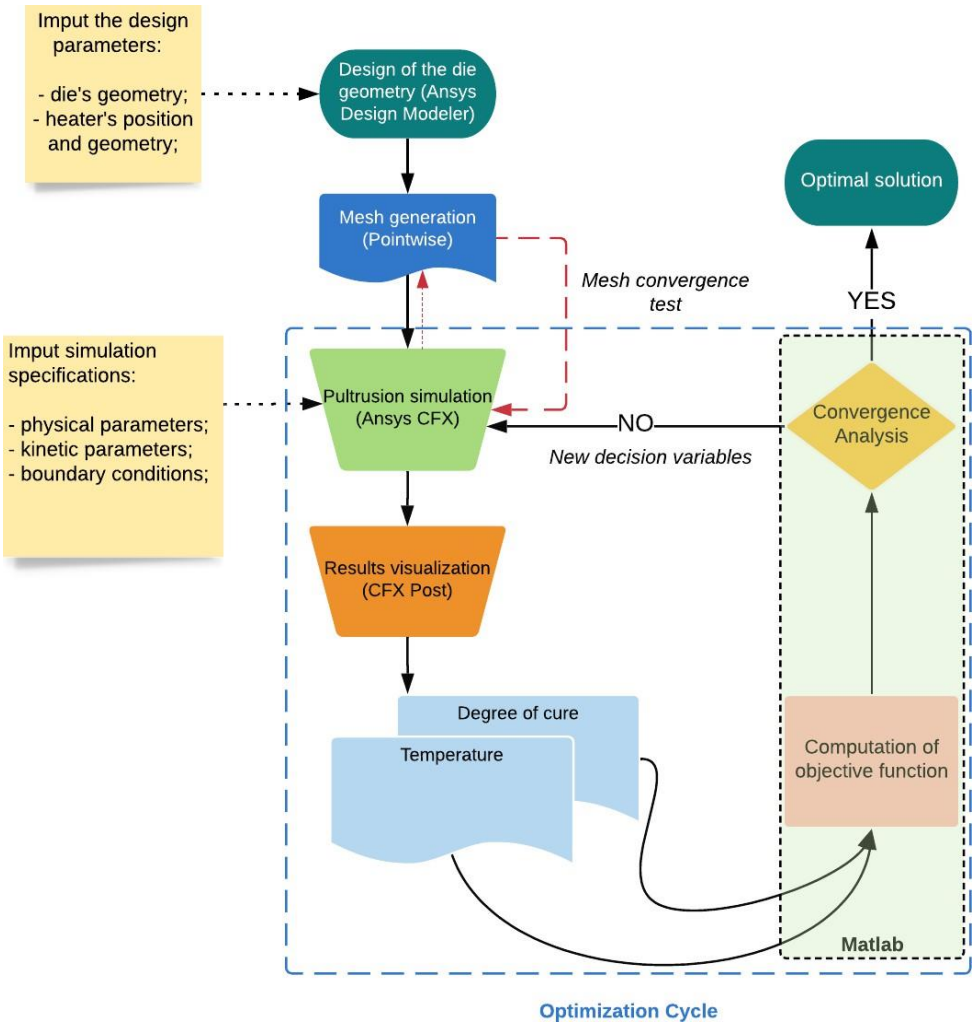

Fig. 2. Flowsheet of the optimization strategy of the pultrusion process.

Algorithm: Optimization strategy

1: Ansys CFX® process simulation.
2: **.def** output file generation.
3: Reading the **.def** file in MATLAB®.
4: Calculate the objective function (with temperature, degree of cure and speed values).
5: Calculation of the values of decision variables.
6: Update the **.def** file.
7: Return to step (1).

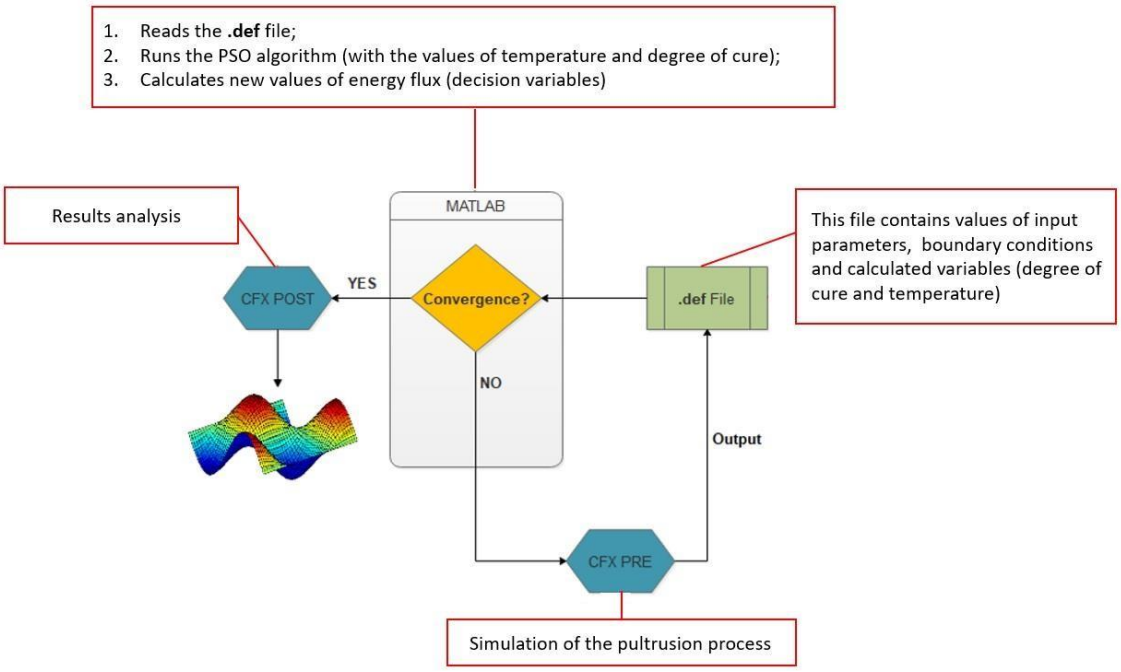

Fig. 3. Flowsheet of the cyclic communication between Matlab®-CFX® softwares.

3. Case Study: Pultrusion of a composite with C-section

3.1 Model description

Pultrusion of a composite C-section is simulated to validate the model studied by Joshi et al. (2003b). The die length, width, and height correspond to 915 mm, 72 and 72 mm, respectively. The heating system comprises six steel heaters with dimensions of 255 mm (length) and 72 mm (width), which are consecutively spaced by 30 mm. The empty zone is subjected to convective boundary conditions. The heaters were positioned in a sequence: (T1, T2, and T3 refer to the heating platens on the top of the die, and T4, T5, and T6 refer to the heating platens on the bottom of the die, in the same order) are shown in Fig. 4. A total 6891 nodes and 27,518 tetrahedral elements were used to create the FE model in Ansys CFX. The material and kinetic parameters are listed in Table 1, and the die and composite dimensions are detailed in Figures 4 and 5, respectively.

Table 1. Process parameters.

Material	ρ (kg/m^3)	c_p (J/Kg · K)	k (W/m · K)
Epoxy resin	1260	1255	0.21
Glass fibers	2560	670	11.4
Crome (5%) steel	7833	460	40

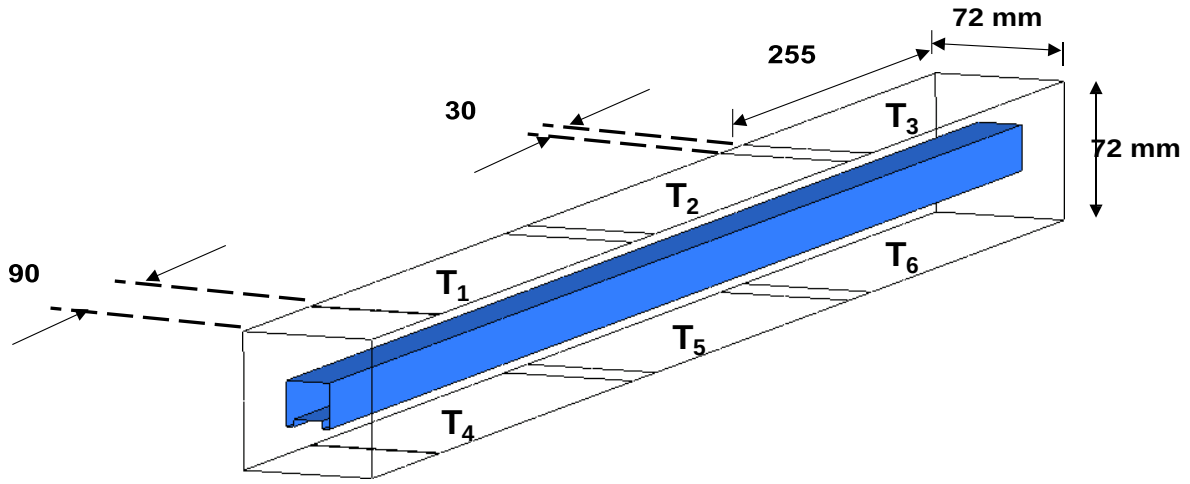

Fig. 4. Case 1:schematic view of pultrusion die.

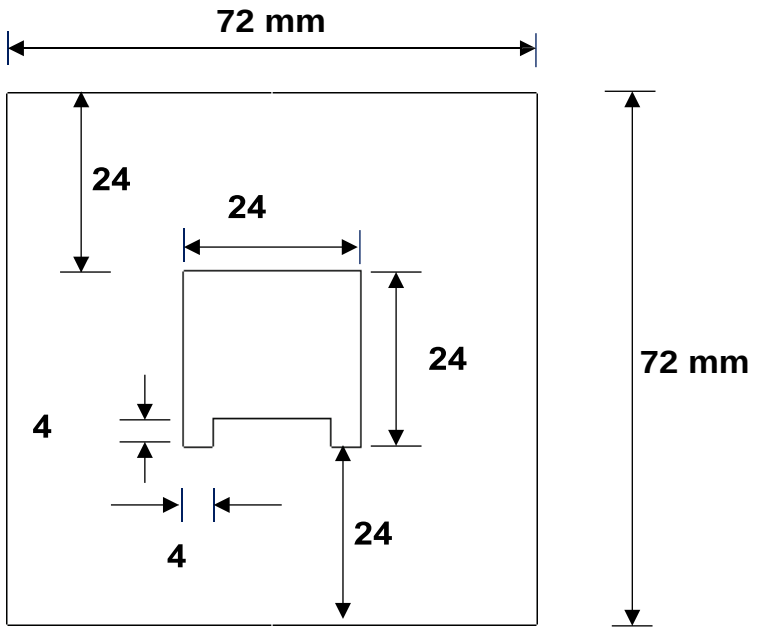

Fig. 5. Case 1:schematic view of pultrusion cavity.

The inlet degree of cure and temperature were considered zero and 298.15 K, respectively. The pultrusion die was considered adiabatic and the temperature distribution and pull speed were set according to the values presented in Table 3.

Table 3. Pull speed and temperature of the simulated process.

F_{obj}	T_1[K]	T_2[K]	T_3[K]	T_4[K]	T_5[K]	T_6[K]	u
2554.4	378.65	421.65	473.15	388.15	419.65	473.15	2.299

3.2 Single-objective Optimization (SOO)

For the PSO algorithm, the strategy of external penalties (Nocedal, 1999) was used to include the constraint of the degree of cure in the objective function. In this case, the optimization problem is formulated according to the following system:

$$\mathbf{min}_{T_{i,\ i=1\cdots n}} \ [\sum_{i=1}^{n} T_i] + \wp \cdot |min\{(0, \alpha - \alpha^*)\}| \tag{5}$$

subject to:

$$\rho_c c_{p_c} \left(\frac{\partial T}{\partial t} + u_z \frac{\partial T}{\partial z}\right) = \nabla(k_c \nabla T) + \frac{dH}{dt} \tag{5a}$$

$$\frac{\partial \alpha}{\partial z} = \rho_r \phi_r H_t r_a \tag{5b}$$

$$r_a = \left(A e^{\left(\frac{-E_a}{RT}\right)}\right)(1-\alpha)^n \tag{5c}$$

where $\wp$ is a constant factor equals 10^3.

For the SQP algorithm (Nocedal, 1999), the minimum cure degree constraint is addressed directly in the optimization problem:

$$\mathbf{min}_{T_{i,\ i=1\cdots n}} \ [\sum_{i=1}^{n} T_i] \tag{6}$$

subject to:

$$\rho_c c_{p_c} \left(\frac{\partial T}{\partial t} + u_z \frac{\partial T}{\partial z}\right) = \nabla(k_c \nabla T) + \frac{dH}{dt} \tag{6a}$$

$$\frac{\partial \alpha}{\partial z} = \rho_r \phi_r H_t r_a \tag{6b}$$

$$r_a = \left(A e^{\left(\frac{-E_a}{RT}\right)}\right)(1-\alpha)^n \tag{6c}$$

$$\alpha \geq \alpha^* \tag{6d}$$

In equations (5) and (6), ρ is the composite density; c_{p_c} is the composite-specific heat; k_c is the composite conductivity; w is the pull speed, z is the pull direction, t is the time and ∇ denotes the gradient operator. The term dH/dt defines the rate of internal heat generation due to cure reaction. H_t represents the total reaction heat per unit mass of resin, ϕ_r is the resin volume fraction,

α is the is degree of cure, B_0 is the pre-exponential constant, ΔE is the activation energy, R is the universal gas constant, n is the reaction order and subscript r denotes resin. $d\alpha/dt$ describes the cure reaction rate.

3.3 Multi-objective Optimization (MOO) applied to Pultrusion Process

In the MOO of the pultrusion process, the goal is to minimize the total temperature and maximize the pull speed. The formulation of the MOO problem is written in equations 7(a-c).

$$\min_{T_{i,\ i=1\cdots n}} [F_{obj}] \tag{7}$$

subject to:

$$\alpha \geq \alpha_{min} \tag{7a}$$

$$\rho_c c_{p_c} \left(\frac{\partial T}{\partial t} + u_z \frac{\partial T}{\partial z}\right) = \nabla (k_c \nabla T) + \frac{dH}{dt} \tag{7b}$$

$$\frac{dH}{dt} = \rho_r \phi_r H_t u_z \frac{\partial \alpha}{\partial z} = \rho_r \phi_r H_t u_z \left[B_0 \cdot \exp\left(\frac{-\Delta E}{RT}\right) \cdot (1-\alpha)^n\right] \tag{7c}$$

where α_{min} corresponds to the minimum degree of cure to be attained (in the center of the composite part).

The multiple objective functions are defined according to equation (8):

$$F_{obj} = \phi F_1 - (1-\phi) F_2 \tag{8}$$

In which $F_1 = \sum_{i=1}^{n} [(T_i - T_{min})/(T_{max} - T_{min})]$ and $F_2 = [(u_{z,i} - u_{z,min})/(u_{z,max} - u_{z,min})]$.

The values of T_{min}, T_{max}, u_{min} and u_{max} were estimated after the solution of the SOO. The parameters of PSO and SQP algorithms as given in the Appendix of this manuscript.

4. Results

4.1. Simulated Results

The temperature and cure profiles in the composite control volume obtained in the simulation are illustrated in Figs. 6 and 7, respectively. By analyzing the temperature profile, it can be noted that the temperature peak of 474.28 K occurs close to the end of the process. It is also clear that the temperature drops slightly close to the die's outlet, characterizing the beginning of the post-cure period. It is known that the temperature peak also occurs due to the exothermic character of the curing reaction, which releases heat throughout the process.

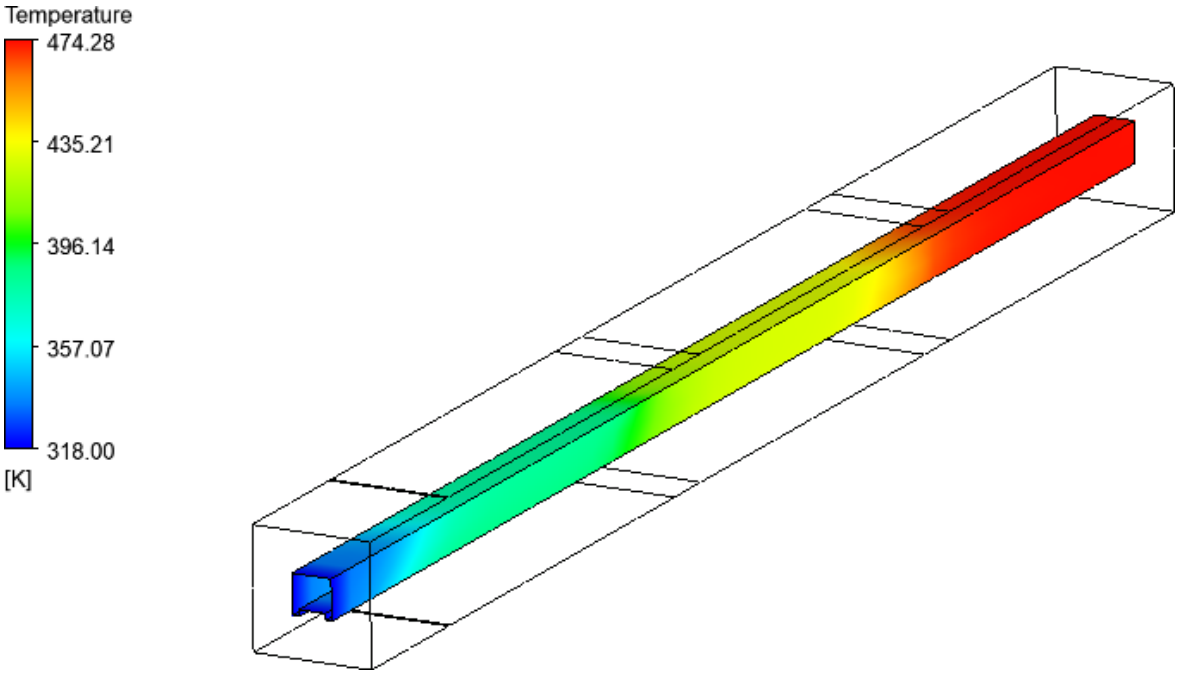

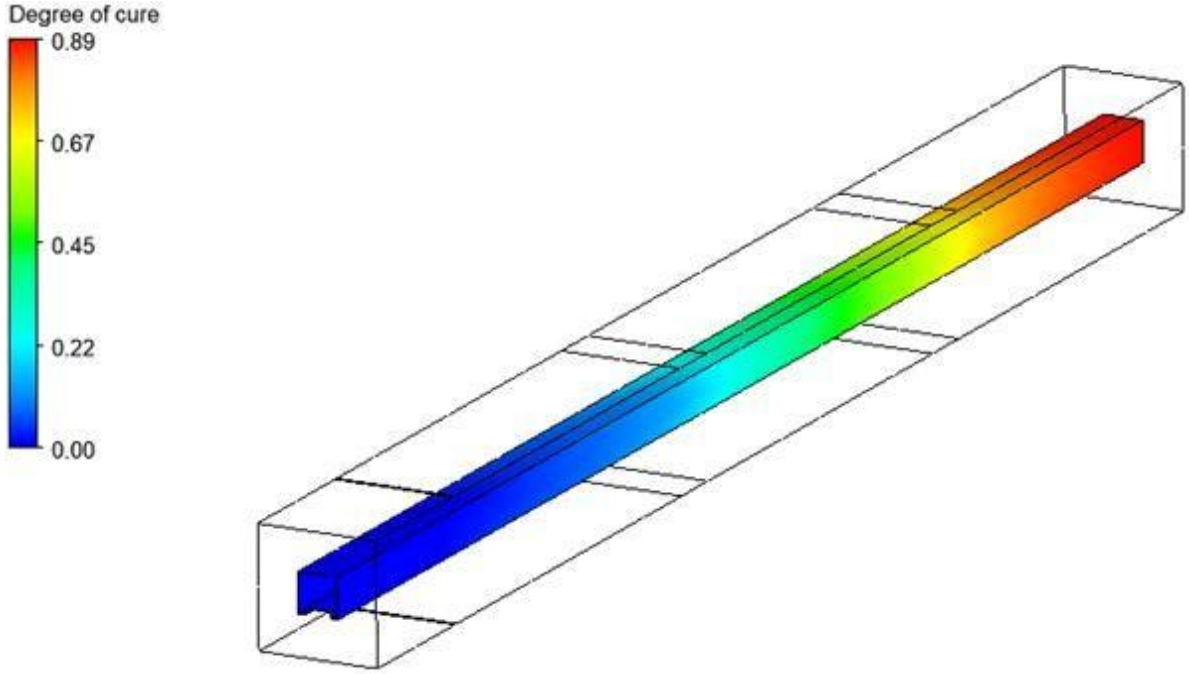

Fig. 6. Simulated temperature profile.

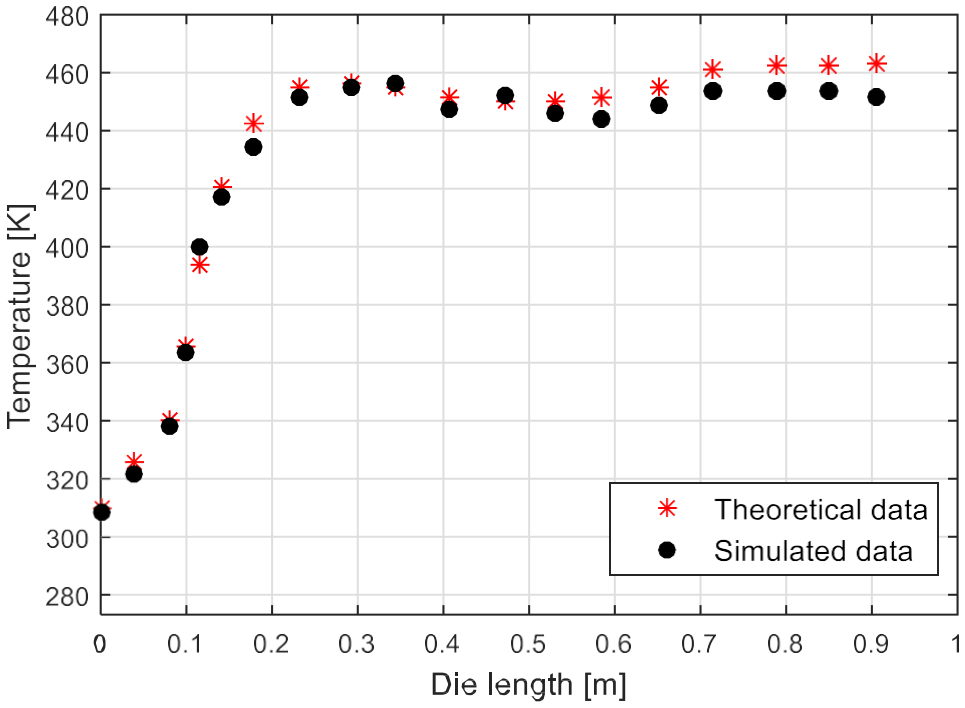

Fig. 7. Simulated and theoretical temperature profiles at the composite centerline.

Fig. 7 shows the simulated and theoretical cure profiles in the centerline of the composite part. Notice that the material achieves the degree of cure of 0.90 at the die exit. It is

possible to observe that both curves have presented a similar tendency, which indicates that the simulated cure profile represents reasonably the theoretical behavior for the considered thermal configuration.

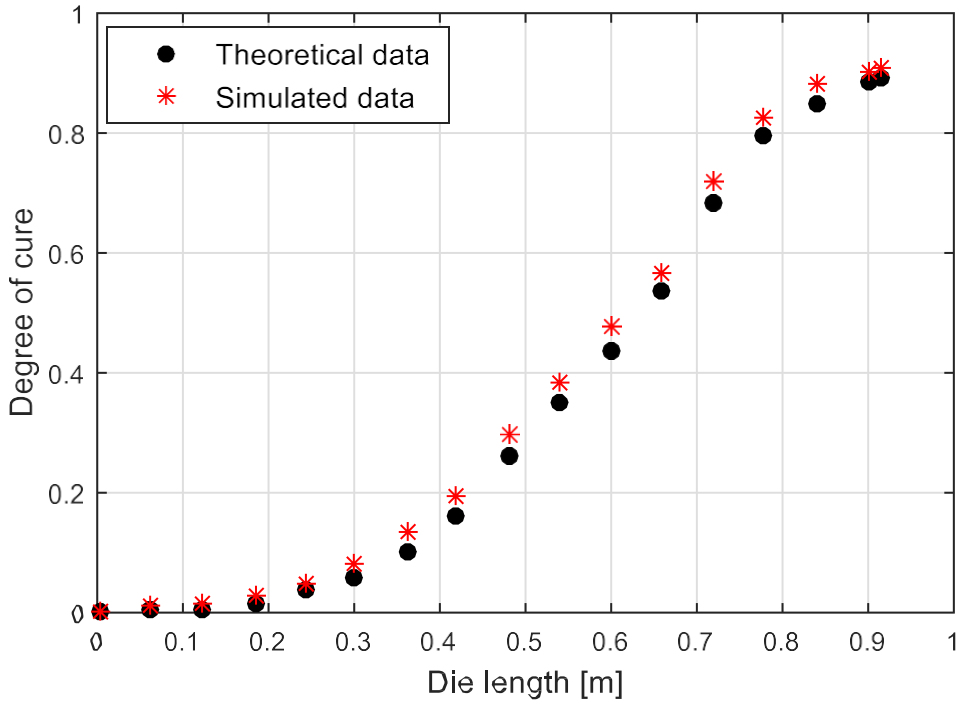

Fig. 8. Simulated and theoretical cure profiles at the composite centerline.

4.2 Sensitivity Analysis

The sensitivity analysis of the objective function and degree of cure concerning the temperature values was performed. The results of this analysis are shown in Figs 7(a-c), where the contour curves referring to the degree of cure were plotted in relation to each heater's temperature pair (upper-lower). Each temperature value was varied for the analysis, keeping the other values constant and equal to the steady-state reference values (Table 3).

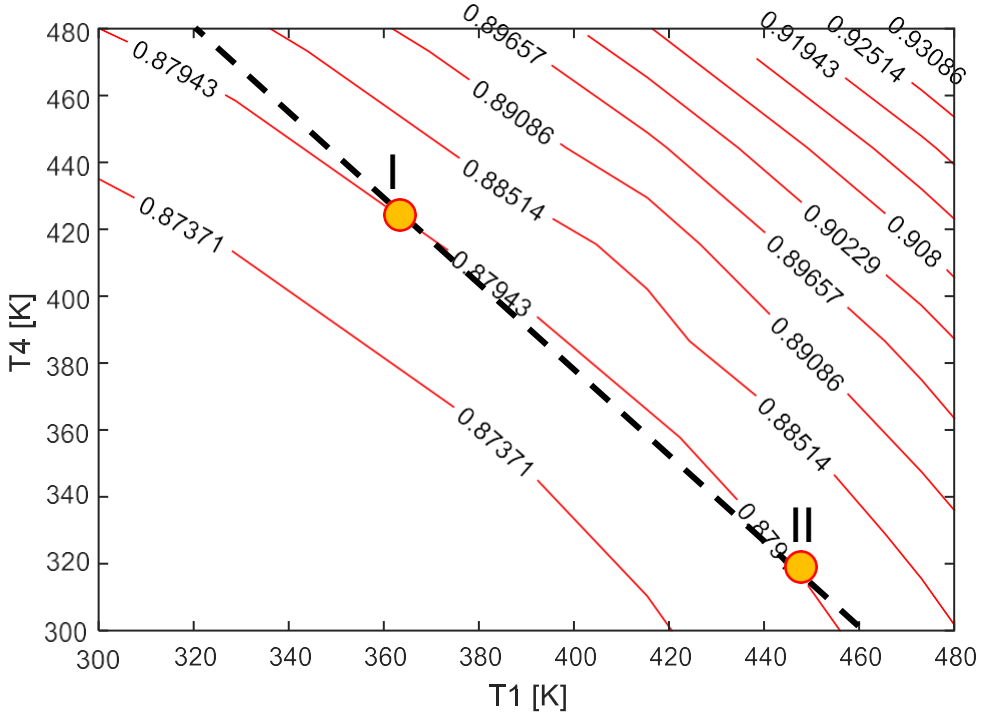

Fig. 7(a) – Contour lines of the degree of cure (red lines) for T1 and T4.

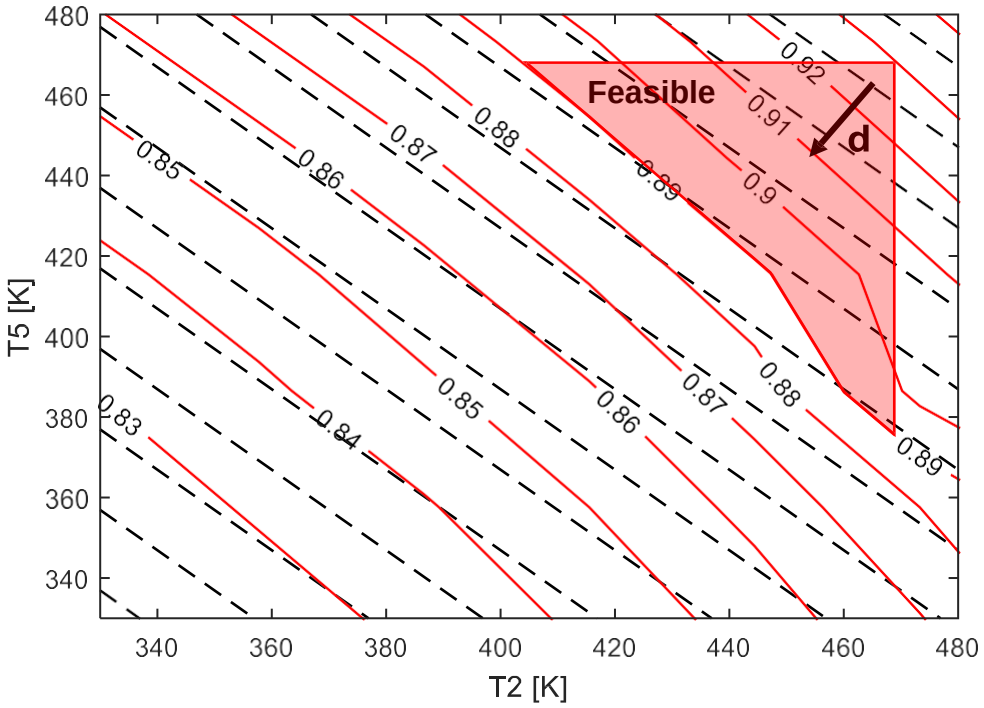

Fig. 7(b) – Contour lines of the objective function (black traced lines) and degree of cure (red lines) for T2 and T5.

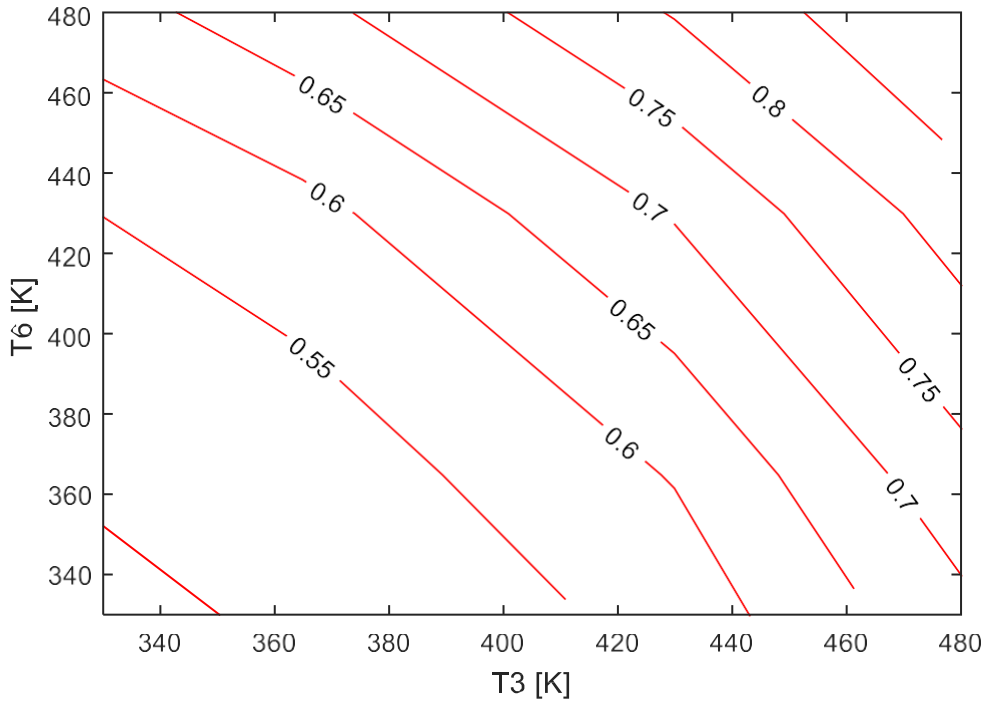

Fig. 7(c) – Contour lines of the degree of cure (red lines) for T3 and T6.

It can be seen in Fig 7(a) that the relationship between the degree of cure and temperatures follows a nonlinear relation, in which the degree of cure increases directly with temperature. In some situations, there is more than one combination of temperatures for a given cure degree value of 0.879. For example, points (I) and (II) have the same degree of cure with different temperature values: point I (T1 = 363.2 K; T4 = 424.1 K) and point II (T1 = 448.7 K; T4 = 320.0 K). It is important to note that these results depend on the other heaters' temperatures.

4.3 Results of Single Objective Optimization

4.3.1 Optimization with Particle Swarm Optimization

As the PSO is a stochastic algorithm, the optimal solution can converge to different points in each optimization computation. Therefore, the PSO was tested for different particle numbers and iteration values to perform the optimization.

Table 4 summarizes the objective function values, temperatures, number of iterations and computational cost for five PSO runs with 30 (3) and 50 (2) iterations.

Table 4. Analysis of the PSO results for 30 and 50 iterations and 15 particles.

Case	F_{obj} (K)	T_1[K]	T_2[K]	T_3[K]	T_4[K]	T_5[K]	T_6[K]	ℓ	CPU(h)
Reference	2554.4	378.65	421.65	473.15	388.15	419.65	473.15	-	-
PSO [1]	**2356.5**	300.00	431.61	473.15	300.00	378.57	473.15	30	7.62
PSO [2]	2451.8	300.00	473.15	432.37	300.00	473.15	473.15	30	7.71
PSO [3]	2420.0	302.20	473.15	472.27	300.00	473.04	399.37	30	7.44
PSO [4]	2447.1	300.83	455.43	464.34	300.00	473.15	453.39	50	10.72
PSO [5]	2442.1	473.15	472.78	300.00	422.92	472.98	300.31	50	10.87
μ_{PSO}	2424.0								8.88
σ_{PSO}	39.7								1.76

Table 3 indicates that the lowest objective function was 2356.5 for case-1. This value corresponds to a 7.74% reduction concerning the reference value ($F_{\text{obj}} = 2554.4$). The highest value of 2451.8 was obtained in case-4. The mean value of the objective functions was 2453.022 and the standard deviation was 39.40. Except for case-5, the solutions indicate that the entrance heaters [1] and [4] present low temperature values.

The average CPU was 7.59 h and 10.80 h for the cases with 30 and 50 iterations, respectively. However, these results indicate that the higher number of iterations did not necessarily correspond to the best solution obtained, as shown in the cases-4 ($F_{\text{obj}} = 2447.1$) and 5 ($F_{\text{obj}} = 2442.1$), which presented objective-function values higher than the values encountered in cases-1 ($F_{\text{obj}} = 2356.5$)and ($F_{\text{obj}} = 2420.0$).

The influence of the number of particles was also evaluated for 15, 20, 25 and 30 particles. This analysis is summarized in Table 5.

Table 5. Influence of the number of particles for 30 iterations.

Particles	F_{obj} (K)	T_1[K]	T_2[K]	T_3[K]	T_4[K]	T_5[K]	T_6[K]	CPU (h)
Reference	2554.4	378.65	421.65	473.15	388.15	419.65	473.15	-
15	**2356.5**	300.00	431.61	473.15	300.00	378.57	473.15	7.62
20	2407.8	300.00	473.00	324.99	303.77	492.98	493.00	8.61
25	2495.2	300.00	473.15	473.15	301.3	475.31	472.31	9.98
30	2403.7	301.12	473.15	475.12	301.7	473.15	473.15	10.65
μ_{PSO}	2434.2							9.21
σ_{PSO}	72.8							1.36

Table 5 shows that the objective-function did not present a crescent variation with the number of particles since the minimum values were encountered with 15 particles ($F_{\text{obj}} = 2356.5$) and the worse value was found with 25 particles ($F_{\text{obj}} = 2495.2$). Nevertheless, the computational cost increased with the number of particles, suggesting that setting this parameter at high values is not advantageous.

Note that the most significant reduction occurred in heaters T1 and T4, representing the heaters close to the inlet region. The heat generated from the exothermic cure reaction probably warmed the system in the initial part of the process. In this way, the optimal strategy suggests that the region enclosed by the two first heaters can be used as a pre-heating phase, in which the heaters are effectively used in the second and third parts of the pultrusion die.

4.3.2 Optimization with Sequential Quadratic Programming (SQP)

In this topic, we present the results of the SQP optimization method. As it is an algorithm based on the computation of the gradient of the objective function, the initial estimative of the decision variables can influence the computed optimal value. Therefore, the system was optimized for five estimation values (in Kelvin). Table 6 summarizes the results for optimization with the use of the SQP algorithm.

Table 6. Analysis of SQP results

Case	F_{obj} (K)	T_1[K]	T_2[K]	T_3[K]	T_4[K]	T_5[K]	T_6[K]	$\mathscr{C}$	CPU (h)
Reference	2554.4	378.65	421.65	473.15	388.15	419.65	473.15	-	-
SQP [1]	2319.2	300.00	473.04	473.01	300.00	300.00	473.13	54	5.31
SQP [2]	2319.2	300.00	473.08	473.02	300.00	300.00	473.13	60	5.78
SQP [3]	2411.4	300.00	468.31	470.53	300.00	417.82	454.77	59	5.67
SQP [4]	2434.4	300.00	473.15	473.15	300.00	473.15	414.99	73	6.41
SQP [5]	2442.8	300.00	448.25	473.15	300.00	473.15	448.23	77	6.23
μ_{SQP}	2385.4							5.78	5.78
σ_{SQP}	61.52							0.37	0.37

In Table 6 the temperature values were estimated according to equation (9):

$$T_k = T_{min} + k \cdot \Delta T \quad (9)$$

In which $\Delta T = (T_{max} - T_{min})/4$ and $k = 1, \cdots, 4$ corresponds to the k^{th} optimization with initial estimative T_k. In the present case, $T_{min} = 300$ K, $T_{max} = 473.15$ K e $\Delta T = 43.2875$ K..

The results evidence that there is a significant influence of the initial temperature estimative on the optimal value computed by the SQP algorithm. The average value of the objective function was 2385.4 K with a standard deviation of 61.52 and an average CPU of 5.78 h. Clearly, the case-1 presented the lowest value of the objective function ($F_{\text{obj}} = 2319.2$), in which 300 K was considered the initial temperature estimate.

4.3.3 Comparison between PSO and SQP algorithms

Table 7 summarizes the best results encountered by the PSO and SQP algorithms. The objective function, temperature values, and computational cost are reported in such analysis.

Table 7. Analysis of SQP and PSO results

Algorithm	F_{obj} (K)	T_1[K]	T_2[K]	T_3[K]	T_4[K]	T_5[K]	T_6[K]	CPU
Reference	2554.4	378.65	421.65	473.15	388.15	419.65	473.15	-
PSO[1]	2356.5	300.00	431.61	473.15	300.00	378.57	473.15	7.62
SQP[1]	2319.2	300.00	473.04	473.01	300.00	300.00	473.13	5.31
RD(%)[1]	-1.58	0.00	+9.60	-0.03	0.00	-20.75	-0.004	-30.31

[1] RD: relative deviation.

The results reported in Table 7 indicate that the SQP algorithm could find an objective function value 1.58% lesser than the value computed by the PSO algorithm. It is also possible to observe that the algorithms showed a similar thermal configuration tendency, with higher temperature values for the (T2, T5) and (T3, T6). However, the optimal values computed for T2 and T5 presented the most significant deviations. The results suggest that the PSO has greater difficulties than the SQP in finding the best solution. However, it is not sensitive to initial estimates, as in the case of the SQP. Therefore, changes in the tuning parameters of the SQP can possibly

improve the success rate in finding the optimal point of the analyzed system. However, the computational cost of the PSO algorithm depends on the configuration of the algorithm parameters, but in the case analyzed the SQP presented a cost 30.31% lower.

4.3.4 Analysis of Temperature and Degree of Cure Profiles

The temperature profiles (measured in the centerline of the composite part) of the composite region are illustrated in the Fig. 8. For comparison, the non-optimal (simulated) temperature profile is also plotted. As observed, in the beginning of the die's entrance, the temperature presents lower values and grows continuously until the exit of the die part. The maximum temperature achieved was approximately 460 K. A considerable difference is noted in the temperature profile of optimal and non-optimal cases. Unlike the non-optimal case, the first heaters had a temperature substantially lower than the heaters of the second zone, as evidenced by the optimization algorithms. The temperature profiles evidence that a more uniform temperature distribution could be obtained in optimal conditions. These results indicate that the optimal energy configuration benefits from the energy released by the cure reaction.

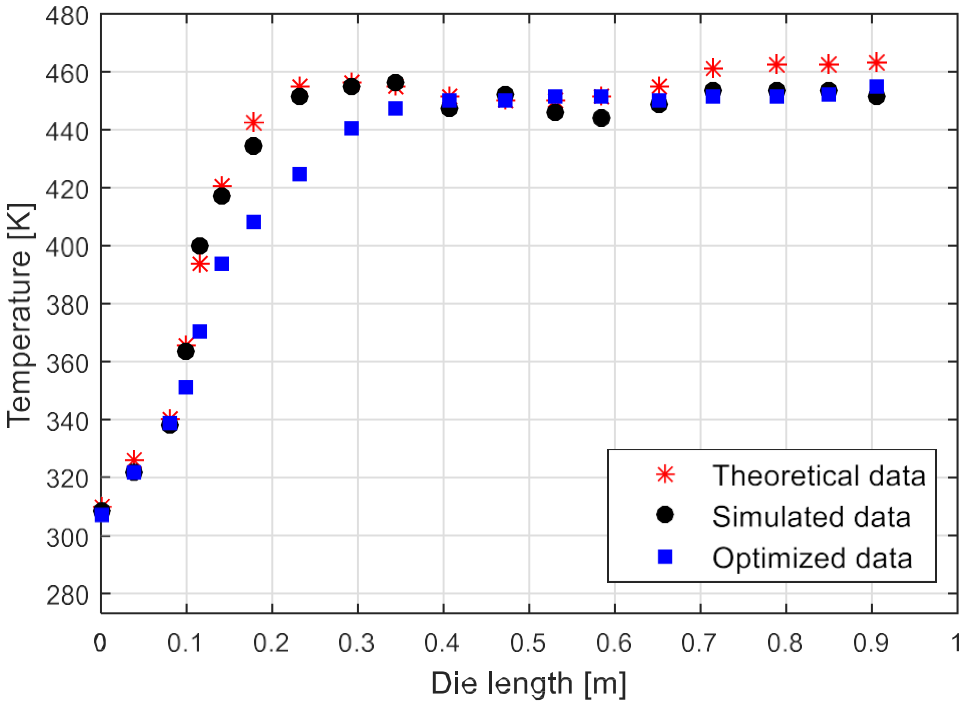

Fig. 8. Optimal temperature profiles centerline of the composite part.

Fig. 9 illustrates the degree of cure profile at the composite's centerline. The degree of cure presents values slightly lower than those obtained in the non-optimal case (simulated data), reaching a value of 0.9 in the outlet section.

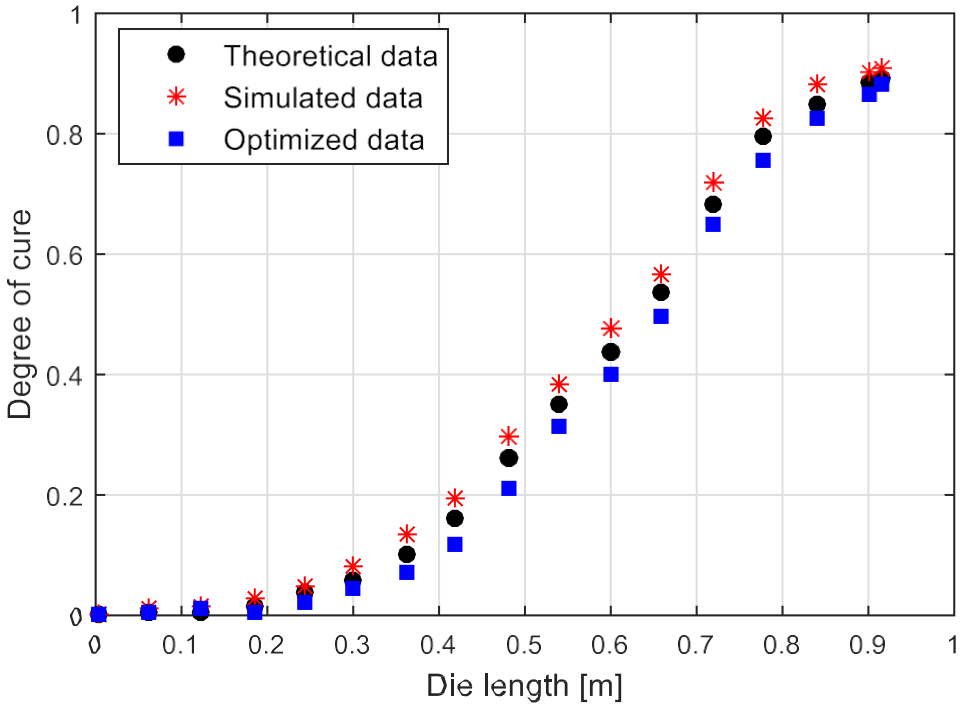

Fig. 9. Optimal cure profiles centerline of the composite part.

4.4 Results of Multi-Objective Optimization

In Fig. 12 each point in the Pareto curve corresponds to an optimal solution found by the PSO-WSM. The curve formed by the optimal points outlines the Pareto boundary that segregates the feasible region (shown above the Pareto curve) from the unfeasible set that does not represent realistic solutions. The Pareto curve can be employed to evaluate all possible optimal solutions and to choose the most feasible one for the process operating conditions.

Notice that the optimal point in the upper left corner corresponds to the maximum sum of dimensionless temperature values that would require greater energy consumption. On the other hand, the right part of the graph corresponds to the lowest values of the dimensionless pull speed. Thus, the intermediate region comprises solutions based on a compromise between the two conflicting objectives. The solution that will be ultimately chosen from the Pareto curve depends

on the engineer's preferences, knowledge about the process, constraints, and decision variables. Therefore, decision-makers must select the most suitable solution based on their experience and context.

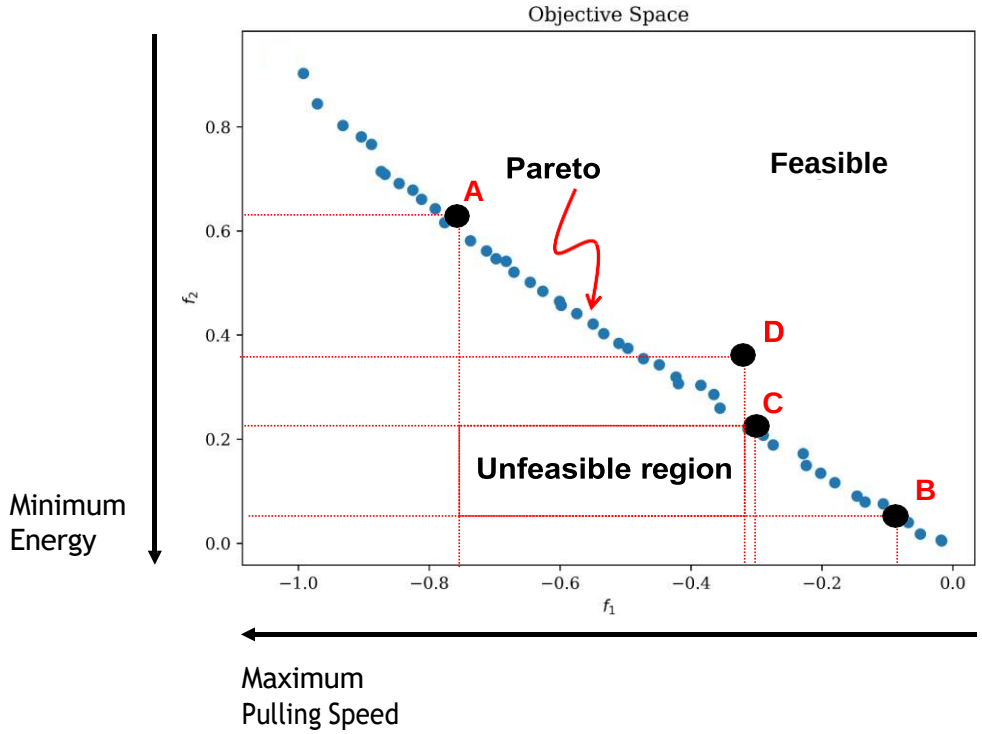

Fig. 12. Pareto curve resulted from the MOO procedure.

To analyze the obtained results, the optimal values were computed for three different points (denoted as A, B and C) on the Pareto curve, as outlined in Fig. 12. Point A represents the highest values of f_1 and f_2, point C represents the intermediate values, and Point B represents the lowest values of f_1 and f_2. Point D corresponds to a non-optimal solution outside the Pareto curve.

Table 9. Analysis of points A, B, C and D

Data	**C**	**B**	**A**	**D**
		OP		NOP
f_1 (dimensionless temperature)	0.31	0.05	0.60	0.37
f_2 (dimensionless pull speed)	0.22	0.08	0.75	0.33

*OP: optimal points; NOP: non-optimal point.

The results reported in Table 9 evidence that the highest dimensionless temperature value (0.63) was obtained at Point A, while the lowest values were obtained at Point B (0.05). As discussed in the previous section, increasing temperature increases energy consumption and pull speed to attain the minimum degree of cure.

Point D can be deemed a feasible solution; however, it does not represent an optimum point since it is not located on the Pareto curve. It is possible to observe that both temperature and pull speed can be optimized from point D by increasing the pull speed or decreasing the temperatures. Table 10 lists the temperature values for each point specified in Fig. 12.

Table 10. Computed temperature and pull speeds for MOO.

Case	F_{obj}	T_1[K]	T_2[K]	T_3[K]	T_4[K]	T_5[K]	T_6[K]	u_z(mm/s)
Reference	2554.4	300.0	439.8	458.6	300.00	452.3	473.15	2.299
A	2495.88	326.41	446.62	473.15	307.61	468.94	473.15	3.90
B	2225.24	300.00	412.3	410.0	300.00	401.63	401.31	2.20
C	2354.95	300.00	410.60	427.00	300.01	456.11	461.23	2.55
D	2382.55	303.10	417.20	434.11	302.41	464.52	461.21	2.82

Fig. 12(a-b) illustrates the cure and temperature profiles for points A, B, C and D.

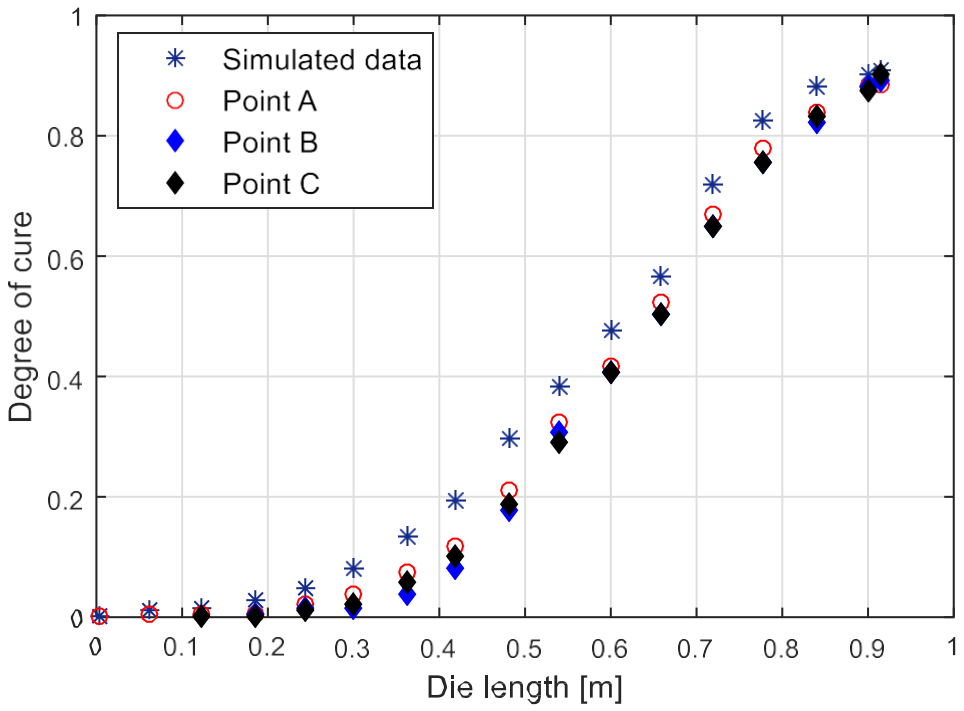

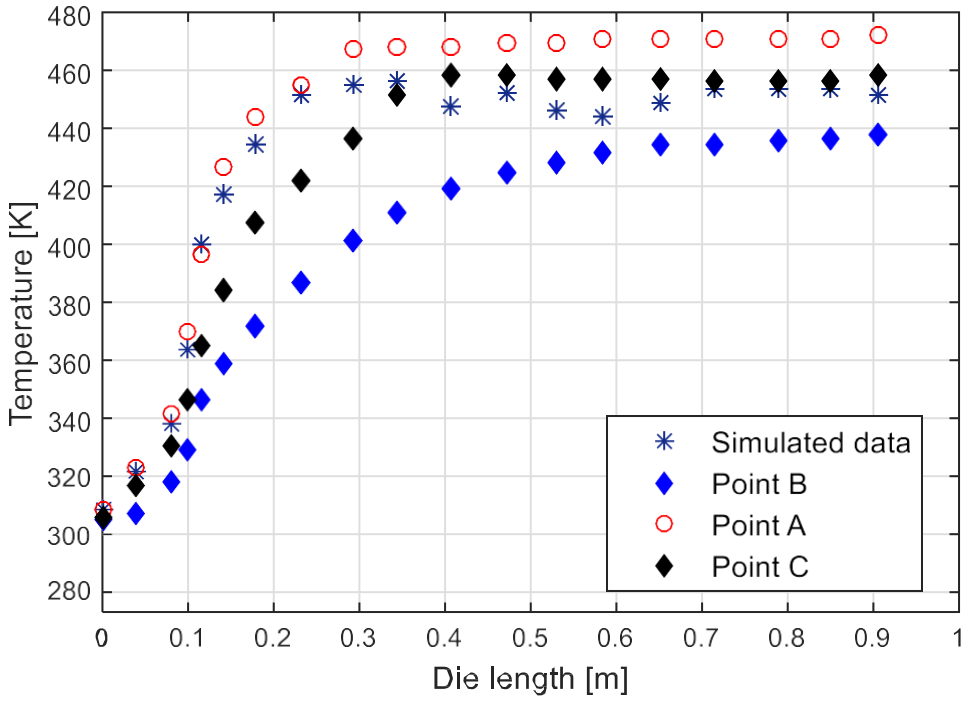

Fig. 12(a) shows that the minimum degree of cure of 0.9 could be attained for four evaluated cases. In addition, the cure profiles presented a similar tendency, indicating that the optimization strategy was able to keep the variables on the optimal Pareto curve. In other words, the temperatures of the heaters are adjusted for each scenario, in which the speed has different values. However, the composite temperature profile has higher values for higher temperature values, as shown in Fig. 12 (b).

5. Conclusions

In this paper, we have developed an optimization strategy that joins Matlab® and ANSYS CFX® solver. The results showed that the PSO algorithm presented higher temperature values than the values calculated by the SQP algorithm. Additionally, the average computational cost of the PSO was 43.50% higher than the cost obtained by the SQP algorithm. However, the SQP was more dependent on initial estimates of heater temperatures.

The multi-objective optimization was performed using the PSO algorithm using the weighted sum strategy to construct the objective function. The Pareto curve of the system could

be obtained, where the optimum values of velocity and temperatures could be obtained. The following results can be highlighted:

1. The simulation performed in the Ansys CFX® software presented satisfactory results, with cure degree and temperature values close to those theoretical results. The proposed Matlab®-Ansys CFX® interface has proved to be a valuable tool for optimizing the system.

2. The PSO and SQP algorithms proved to be efficient methods to optimize the cure cycle. According to the reported results, it was possible to minimize the rate of energy consumed and increase production. Besides, the results showed that the cure could be better distributed throughout the process.

Nomenclature

Acronyms

CFD	Computational Fluid Dynamics
GA	Genetic Algorithm
OA	Optimization Algorithm
PDE	Partial Differential Equations
PSO	Particle Swarm Optimization
SA	Simulated Annealing
SD	Steepest Descent
SOO	Single Objective Optimization
SQP	Sequential Quadratic Programming
MOO	Multi-objective Optimization
NSGA-II	Non Sorting Genetic Algorithm
WSM	Weight Sum Method

Latin letters

A	Activation energy
c	Specific heat
E_a	Activation Energy

g	Inequality constraints
h	Equality constraints
H	Enthalpy
k	Thermal conductivity
$Fobj$	Objective function
R	Universal gas constant
T	Temperature
u	Pull speed
r_a	Kinetic rate
x	Decision variables
z	Pull direction

Greek letters

α	Degree of cure
$\wp$	Penalty parameter
ρ	Density
ϕ	Volume fraction s

Mathematical notation

max	Maximization
min	Minimization

Indices, subscripts and superscripts

$(\cdot)_{min}$	Lower bound
$(\cdot)_{max}$	Upper bound
$(\cdot)_r$	Resin
$(\cdot)_f$	Fiber
$(\cdot)_C$	Composite
$(\cdot)_t$	Total

7. References

Acquah, C., Datskov, I., Mawardi, A., Zhang, F., Achenie, L.E.K., Pitchumani, R., Santos, E., 2006. Optimization under uncertainty of a composite fabrication process using a deterministic one-stage approach. Comput Chem Eng 30, 947–960. https://doi.org/10.1016/j.compchemeng.2005.12.015

Biegler, L., 2010. Nonlinear programming: concepts, algorithms, and applications to chemical processes.

Carlone, P., Palazzo, G.S., Pasquino, R., 2007. Pultrusion manufacturing process development: Cure optimization by hybrid computational methods. Computers and Mathematics with Applications 53, 1464–1471. https://doi.org/10.1016/j.camwa.2006.02.031

Chapra, S.C., Canale, R.P., 2003. Numerical methods for engineers, Mathematics and Computers in Simulation. McGraw-Hill Science/Engineering/Math. https://doi.org/10.1016/0378-4754(91)90127-o

Coelho, R.M.L., Calado, V.M.A., 2002. An optimization procedure for the pultrusion process based on a finite element formulation. Polym Compos 23, 329–341. https://doi.org/10.1002/pc.10435

Costa, R.D.C.D., Santos, L. de S., Ouzia, H., Schledjewski, R., 2018. Improving degree of cure in pultrusion process by optimizing die-temperature. Mater Today Commun 17, 362–370. https://doi.org/10.1016/j.mtcomm.2018.08.017

Joshi, S.C., Lam, Y.C., Win Tun, U., 2003a. Improved cure optimization in pultrusion with pre-heating and die-cooler temperature. Compos Part A Appl Sci Manuf 34, 1151–1159. https://doi.org/10.1016/j.compositesa.2003.08.003

Joshi, S.C., Lam, Y.C., Win Tun, U., 2003b. Improved cure optimization in pultrusion with pre-heating and die-cooler temperature. Compos Part A Appl Sci Manuf 34, 1151–1159. https://doi.org/10.1016/J.COMPOSITESA.2003.08.003

Lam, Y.C., Jianhua Li, Joshi, S.C., 2003. Simultaneous optimization of die-heating and pull-speed in pultrusion of thermosetting composites. Polym Compos 24, 199–209. https://doi.org/10.1002/pc.10020

Li, J., Joshi, S.C., Lam, Y.C., 2002. Curing optimization for pultruded composite sections. Compos Sci Technol 62, 457–467. https://doi.org/10.1016/S0266-3538(02)00018-0

Nickels, L., 2019. The future of pultrusion. Reinforced Plastics xxx, 1–4. https://doi.org/10.1016/j.repl.2019.01.003

Nocedal, J., 1999. Numerical Optimization. https://doi.org/10.1007/BF01068601

Pardalos, P.M., Žilinskas, A., Žilinskas, J., 2017. Springer Optimization and Its Applications 123 Non-Convex Multi-Objective Optimization. Springer International Publishing, Gewerbestrasse.

Safonov, A.A., Carlone, P., Akhatov, I., 2018. Mathematical simulation of pultrusion processes: A review. Compos Struct 184, 153–177. https://doi.org/10.1016/j.compstruct.2017.09.093

Santos, L.S., Biscaia, E.C., Pagano, R.L., Calado, V.M.A., 2012. CFD-OPTIMIZATION ALGORITHM TO OPTIMIZE THE ENERGY TRANSPORT IN PULTRUDED POLYMER COMPOSITES. Brazilian Journal of Chemical Engineering. https://doi.org/10.1590/S0104-66322012000300013

Santos, L.S., Pagano, R.L., Biscaia, E.C., Calado, V.M.A., 2009. Optimum Heating Configuration of Pultrusion Process. 10th International Symposium on Process Systems Engineering.

Santos, L.S., Pagano, R.L., Calado, V.M.A., Biscaia, E.C., 2015a. Optimization of a pultrusion process using finite difference and particle swarm algorithms. Brazilian Journal of Chemical Engineering. https://doi.org/10.1590/0104-6632.20150322s00003181

Santos, L.S., Pagano, R.L., Calado, V.M.A., Biscaia Jr, E.C., 2015b. OPTIMIZATION OF A PULTRUSION PROCESS USING FINITE DIFFERENCE AND PARTICLE SWARM ALGORITHMS. Brazilian Journal of Chemical Engineering.

Silva, F.J.G., Ferreira, F., Ribeiro, M.C.S., Castro, A.C.M., Castro, M.R.A., Dinis, M.L., Fiúza, A., 2014. Optimising the energy consumption on pultrusion process. Compos B Eng 57, 13–20. https://doi.org/10.1016/j.compositesb.2013.09.035

Srinivasagupta, D., Kardos, J.L., 2004. Ecologically and economically conscious design of the injected pultrusion process via multi-objective optimization. Model Simul Mat Sci Eng 12. https://doi.org/10.1088/0965-0393/12/3/S10

Struzziero, G., Teuwen, J.J.E., Skordos, A.A., 2019. Numerical optimisation of thermoset composites manufacturing processes: A review. Compos Part A Appl Sci Manuf 124, 105499. https://doi.org/10.1016/j.compositesa.2019.105499

Tutum, C.C., Baran, I., Deb, K., 2014. Optimum design of pultrusion process via evolutionary multi-objective optimization. International Journal of Advanced Manufacturing Technology 72, 1205–1217. https://doi.org/10.1007/s00170-014-5726-6

Tutum, C.C., Baran, I., Hattel, J., 2013. Utilizing Multiple Objectives for the Optimization of the Pultrusion Process Based on a Thermo-Chemical Simulation, in: The Current State-of-the-Art on Material Forming, Key Engineering Materials. Trans Tech Publications Ltd, pp. 2165–2174. https://doi.org/10.4028/www.scientific.net/KEM.554-557.2165

Tutum, C.C., Deb, K., Baran, I., 2015. Constrained efficient global optimization for pultrusion process. Materials and Manufacturing Processes 30, 538–551. https://doi.org/10.1080/10426914.2014.994752

Wilcox, J.A.D., Wright, D.T., 1998. Towards pultrusion process optimisation using artificial neural networks. J Mater Process Technol 83, 131–141. https://doi.org/10.1016/S0924-0136(98)00052-1

Appendix A – Parameters of Optimization Algorithms

(A1) Particle Swarm Optimization

Particle Swarm Optimization (PSO) is an evolutionary algorithm developed by Kennedy and Eberhart (1995) based on the simulation of the social behavior of a flock of birds during flight. Each bird makes an analogy to a candidate for the optimization problem's solution, called a particle. Particles evolve over the iterations in the search for the optimum, only through competition and cooperation between them, without considering genetic operators (Marini e Walczak, 2015).

Regarding n_z particles, one single particle i has the position $\boldsymbol{z_i} = [z_{i1}, z_{i2}, \dots, z_{i,n_z}]$ and velocity $\boldsymbol{v_i} = [v_{i1}, v_{i2}, \dots, v_{i,n_z}]$, in which n_z is the dimension of the optimization problem. Considering two successive iterations k e $k + 1$, the values of $\boldsymbol{z_i}$ and $\boldsymbol{v_i}$ are computed according to equations (2) and (3), respectively:

$$\boldsymbol{z_i^{k+1}} = \boldsymbol{z_i^{k}} + \boldsymbol{v_i^{k+1}} \quad \text{(A1)}$$

$$\boldsymbol{v_i^{k+1}} = \lambda v_i^{k} + c_1 R_1 (p_{g,i}^{k} - z_i^{k}) + c_2 R_2 (g_{g,i}^{k} - z_i^{k}) \quad \text{(A2)}$$

In which $p_{g,i}$ is the best position encountered by the particle i, $g_{g,i}$ is the best position regarding all particles, R_1 and R_2 are random numbers regarding a uniform distribution [0,1]; $c_1 = 2$ and $c_2 = 2$ are acceleration constants. The inertia parameter λ is written according to equation (4).

$$\lambda(t) = \lambda_{max} - \frac{\lambda_{max} - \lambda_{min}}{t_{max}} \cdot t \quad \text{(A3)}$$

where λ_{max} e λ_{min} are the maximum and minimum values and k_{max} is the maximum number of iterations.

Table A lists the PSO parameters.

Table A. PSO parameters.

Parameter	Valu
Number of iteration	100
Population size	100
Crossover probabilit	0.9
Mutation probabilit	0.01

(A2) Sequential Quadratic Programming

Table B. SQP Parameters

Description	Value	Observations
Constraints tolerance	10^{-6}	SQP algorithm
Objective function tolerance	10^{-6}	SQP algorithm
State tolerance	10^{-6}	SQP algorithm

Declaration of interests

☒ The authors declare that they have no known competing financial interests or personal relationships that could have appeared to influence the work reported in this paper.

☐ The authors declare the following financial interests/personal relationships which may be considered as potential competing interests:

Author Agreement Statement

We the undersigned declare that this manuscript is original, has not been published before and is not currently being considered for publication elsewhere. We confirm that the manuscript has been read and approved by all named authors and that there are no other persons who satisfied the criteria for authorship but are not listed. We further confirm that the order of authors listed in the manuscript has been approved by all of us. We understand that the Corresponding Author is the sole contact for the Editorial process. He is responsible for communicating with the other authors about progress, submissions of revisions and final approval of proofs.

Manuscript: Analysis of single and multi-objective optimization of the pultrusion process

First author: Rita de Cassia Costa Dias

Second author: Lizandro de Sousa Santos

Corresponding author: Lizandro de Sousa Santos <lizandrosousa@id.uff.br>

CRediT author statement

Lizandro de Sousa Santos: Conceptualization, Methodology, Optimization, Writing- Reviewing and Editing.

Rita de Cassia Costa Dias: Modeling, Simulation, Validation, Writing-Reviewing and Editing.